

BASIC SCIENCES

ALDH2 (Aldehyde Dehydrogenase 2) Protects Against Hypoxia-Induced Pulmonary Hypertension

Yu Zhao, Bailu Wang, Jian Zhang, Dayu He, Qun Zhang, Chang Pan, Qihuan Yuan, Yinan Shi, Haiyang Tang, Feng Xu, Shujian Wei, Yuguo Chen

OBJECTIVE: Hypoxia-induced pulmonary hypertension (HPH) increases lipid peroxidation with generation of toxic aldehydes that are metabolized by detoxifying enzymes, including ALDH2 (aldehyde dehydrogenase 2). However, the role of lipid peroxidation and ALDH2 in HPH pathogenesis remain undefined.

APPROACH AND RESULTS: To determine the role of lipid peroxidation and ALDH2 in HPH, C57BL/6 mice, ALDH2 transgenic mice, and ALDH2 knockout (ALDH2^{-/-}) mice were exposed to chronic hypoxia, and recombinant tissue-specific ALDH2 overexpression adeno-associated viruses were introduced into pulmonary arteries via tail vein injection for ALDH2 overexpression. Human pulmonary artery smooth muscle cells were used to elucidate underlying mechanisms in vitro. Chronic hypoxia promoted lipid peroxidation due to the excessive production of reactive oxygen species and increased expression of lipoxygenases in lung tissues. 4-hydroxynonenal but not malondialdehyde level was increased in hypoxic lung tissues which might reflect differences in detoxifying enzymes. ALDH2 overexpression attenuated the development of HPH, whereas ALDH2 knockout aggravated it. Specific overexpression of ALDH2 using AAV1 (adeno-associated virus)-ICAM (intercellular adhesion molecule) 2p-ALDH2 and AAV2-SM22 α (smooth muscle 22 alpha)-ALDH2 viral vectors in pulmonary artery smooth muscle cells, but not endothelial cells, prevented the development of HPH. Hypoxia or 4-hydroxynonenal increased stabilization of HIF (hypoxia-inducible factor)-1 α , phosphorylation of Drp1 (dynamin-related protein 1) at serine 616, mitochondrial fission, and pulmonary artery smooth muscle cells proliferation, whereas ALDH2 activation suppressed the latter 3.

CONCLUSIONS: Increased 4-hydroxynonenal level plays a critical role in the development of HPH. ALDH2 attenuates the development of HPH by regulating mitochondrial fission and smooth muscle cell proliferation suggesting ALDH2 as a potential new therapeutic target for pulmonary hypertension.

VISUAL OVERVIEW: An online [visual overview](#) is available for this article.

Key Words: hypoxia ■ lipid peroxidation ■ mitochondrial fission ■ pulmonary artery ■ pulmonary hypertension

Pulmonary hypertension (PH) is a vascular disease characterized by resting mean pulmonary artery pressure ≥ 25 mm Hg.¹ Hypoxia-induced PH (HPH), one of the most common types of PH, is frequently found in patients with chronic hypoxic lung diseases, including chronic obstructive pulmonary disease, obstructive sleep apnea syndrome, interstitial lung disease, bronchiectasis, and chronic mountain sickness.^{2,3}

The development of HPH is associated with worsening symptoms and poor prognosis due to elevated pulmonary artery pressure, right ventricular hypertrophy (RVH), and failure eventually.⁴ Long-term oxygen therapy in chronic obstructive pulmonary disease is effective in prolonging survival but only reduces pulmonary arterial pressure mildly.⁵ Up to now, no targeted drugs including pulmonary vasodilators have shown effectiveness in

Correspondence to: Feng Xu, MD, PhD, Department of Emergency, Qilu Hospital, Shandong University, Jinan 250012, China, Email xufengsdu@126.com; or Shujian Wei, MD, PhD, Department of Emergency, Qilu Hospital, Shandong University, Jinan 250012, China, Email weishujian@sdu.edu.cn; or Yuguo Chen, MD, PhD, Department of Emergency, Qilu Hospital, Shandong University, Jinan 250012, China, Email chen919085@sdu.edu.cn

The online-only Data Supplement is available with this article at <https://www.ahajournals.org/doi/suppl/10.1161/ATVBAHA.119.312946>.

For Sources of Funding and Disclosures, see page 2318.

© 2019 American Heart Association, Inc.

Arterioscler Thromb Vasc Biol is available at www.ahajournals.org/journal/atvb

Nonstandard Abbreviations and Acronyms

4-HNE	4-hydroxynonenal
8-iso-PGF2α	8-iso-prostaglandin F2 alpha
ADH	alcohol dehydrogenase
AKR	aldo-keto reductases
ALDH1A1	aldehyde dehydrogenase family 1 member A1
ALDH2	aldehyde dehydrogenase 2
AO	aldehyde oxidase
AP-1	activating protein 1
CDK1	cyclin-dependent kinase 1
Drp1	dynamamin-related protein 1
FIS1	mitochondrial fission protein 1
GST	glutathione S-transferase
HIF-1α	hypoxia-inducible factor-1 α
HPASMCs	human pulmonary artery smooth muscle cells
HPH	hypoxia-induced pulmonary hypertension
LO	lipoyxygenase
MFN	mitofusin
NAC	N-acetyl-L-cysteine
NF	nuclear factor
NOXs	nicotinamide adenine dinucleotide phosphate oxidases
Nrf2	nuclear factor erythroid 2-related factor 2
OPA1	optic atrophy protein 1
PASMCs	pulmonary artery smooth muscle cells
PPAR	peroxisome-proliferator-activated receptor
ROS	reactive oxygen species
RVH	right ventricular hypertrophy
RVSP	right ventricular systolic pressure

the treatment of HPH.⁶ Thus, gaining insight into the underlying mechanisms of HPH is necessary to identify potential new therapeutic targets.

Chronic exposure to hypoxia induces inflammation, vasoconstriction, smooth muscle cell proliferation, muscularization of precapillary arterioles, and loss of distal pulmonary vessels, which are the key pathophysiological processes in HPH.^{3,5} Although thickening of all the layers of the walls of the pulmonary vessels contributes to HPH, media remodeling plays a predominant role in its development.⁷ Pulmonary artery smooth muscle cells (PASMCs) are the primary cells of the arterial medial layer. Hypoxia induces excessive PASMCs proliferation, with HIF (hypoxia-inducible factor)-1 α playing a critical role in regulating the transcription of hypoxia-specific genes.⁹ HIF-1 α is an oxygen-regulated subunit of the

Highlights

- Increased lipid peroxidation contributes to the development of hypoxia-induced pulmonary hypertension. 4-hydroxynonenal, but not malondialdehyde, is increased in hypoxic lung tissues.
- As the detoxifying enzyme of 4-hydroxynonenal, ALDH2 (aldehyde dehydrogenase 2) prevents hypoxia-induced pulmonary hypertension.
- ALDH2 regulates mitochondrial fission and smooth muscle cells proliferation via 4-hydroxynonenal/HIF (hypoxia-inducible factor)-1 α /Drp1 (dynamamin-related protein 1) signal pathway.

heterodimeric transcription factor-HIF that is degraded and inactivated via hydroxylation of specific prolyl and asparaginyl residues under normal conditions but is significantly upregulated under hypoxia.⁹

Hypoxia causes excessive production of reactive oxygen species (ROS) that originate from mitochondria and NOXs (nicotinamide adenine dinucleotide phosphate oxidases)¹⁰ and attack and promote the oxidation of lipids, especially polyunsaturated fatty acids, a process termed lipid peroxidation.¹¹ Lipid peroxidation produces a wide variety of oxidation products among which aldehydes are the major end products.¹¹ Toxic aldehydes are highly reactive and interact with cellular macromolecules, including nucleic acids and proteins to generate various adducts, resulting in DNA damage and inactivation of proteins.¹² Among products of lipid peroxidation, 4-hydroxynonenal (4-HNE) is thought to be the most toxic aldehyde and malondialdehyde appears to be the most mutagenic aldehyde.¹¹ Oxidized lipids have been involved in PASMCs proliferation and exacerbate the development of HPH; however, it remains undefined if production of toxic aldehydes contribute to vascular modeling in HPH.¹³

Aldehydes are mainly metabolized and detoxified by ALDHs (aldehyde dehydrogenases), AO (aldehyde oxidase), AKR (Aldo-keto reductases), and GSTs (glutathione S-transferases).¹⁴ ALDHs are a superfamily that includes 19 subtypes in humans.¹⁵ ALDH2 is the mitochondrial isoform of ALDH and is a key metabolizer of acetaldehyde.¹⁶ ALDH2 is a protective factor in myocardial damage and stroke by clearing toxic aldehydes generated from lipid peroxidation, especially 4-HNE.^{17,18} Although a previous study demonstrated that ALDH2 activation alleviates monocrotaline-induced pulmonary arterial hypertension, the role of ALDH2 in HPH and its underlying mechanisms are largely unexplored.¹⁹

In the present study, we found that chronic hypoxia promoted the production of 4-HNE in lung tissue. Using multiple approaches, we demonstrated that ALDH2 activation reduced the level of 4-HNE, attenuated the severity of HPH in vivo and regulated PASMCs proliferation and migration in vitro.

METHODS

The data that support the findings of this study are available from the corresponding author upon reasonable request.

Animal Models

C57BL/6J (wide-type) mice, ALDH2^{-/-} mice, ALDH2-Tg (ALDH2 transgenic) mice, and their littermates (10–12 weeks) weighing 20 to 25 g were used in this study. C57BL/6J mice were purchased from the Department of Experimental Animals of Shandong University (Jinan, China). ALDH2^{-/-} mice were provided by University of Occupational and Environmental Health (Fukuoka, Japan). ALDH2-Tg mice were gifts from Professor Jun Ren (University of Wyoming). Mice were either placed in normal air or in a normobaric hypoxic chamber (FiO₂ 10%) for 3 weeks. To avoid the potential effects of estrogen on PH, age-matched male but not female littermates were used in this study. 4-HNE was administered with miniosmotic pumps (0.19 mg/kg per hour) or peritoneal injection every day (10 mg/kg). Alda-1 (15 mg/kg, MedChemExpress) was intraperitoneally injected every day. N-acetyl-L-cysteine (NAC) treatment was administered with a dose of 160 mg/kg by oral gavage once daily. For Sugen/hypoxia PH model, C57BL/6J mice were subcutaneously injected with Sugen 5416 (20 mg/kg, Cayman Chemicals) once a week and exposed to normobaric hypoxic chamber (FiO₂ 10%) for 3 weeks and then were intraperitoneally injected with Alda-1 (15 mg/kg) or vehicle every day for 2 more weeks.²⁰ All animal procedures were in accordance with the National Institutes of Health Guidelines and were approved by the Animal Use and Care Committee of Shandong University.

Hemodynamic and Ventricular Weight Measurements

After mice were weighed and anesthetized, right ventricular systolic pressure (RVSP) was measured by direct cardiac puncture using 23G needle attached to a pressure transducer, and data were collected and analyzed using the PowerLab Software (ADI Instruments, Colorado Springs, CO). RVH was estimated by Fulton index (the weight ratio of right ventricle/septum with left ventricle).

4-HNE, Malondialdehyde, and 8-Iso-Prostaglandin F2 Alpha Assays

Plasma 4-HNE was assessed using a 4-HNE ELISA Kit (Meimian, Jiangsu, China). Plasma and tissue malondialdehyde was evaluated with a Lipid Peroxidation (malondialdehyde) Assay Kit (Abcam, ab118970, Cambridge, MA). Plasma level of 8-iso-prostaglandin F2 alpha (8-iso-PGF2 α) was determined using 8-iso-PGF2 α ELISA Kit (ab133043; Abcam). All experiments were performed according to the manufacturer's instructions.

Human Samples

Human lung tissues were obtained from autopsied patients or patients underwent thoracic surgery in Qilu Hospital of Shandong University (Table I in the [online-only Data Supplement](#)). Human plasma samples were from patients with

PH (moderate/severe) or without PH (Table II in the [online-only Data Supplement](#)). Written consent was obtained from all the participants. This study was performed in accordance with the Helsinki Doctrine on Human Experimentation and was approved by the Ethics Review Committee of Qilu Hospital of Shandong University.

Cell Culture

Human pulmonary artery smooth muscle cells (HPASMCs) were purchased from American Type Cell Collection (Manassas, VA) and PSMCs isolated from idiopathic pulmonary arterial hypertension or normal subjects were obtained from Pulmonary Hypertension Breakthrough Initiative (Philadelphia, PA). Cells were grown in Vascular Cell Basal Medium (ATCC, PCS-100030, Manassas, VA) plus Vascular Smooth Muscle Cell Growth Kit (ATCC, PCS100042, Manassas, VA). The cells were cultured under normal oxygen tension (20% O₂, 5% CO₂) or exposed to hypoxia (2% O₂, 5% CO₂, 92% N₂) at 37°C in a humidified atmosphere. For stimulation, fresh medium containing different concentrations of 4-HNE (0.1 μ M, 1 μ M, 10 μ M), alda-1 (20 μ M), or daidzin (60 μ M) was added to microplates, and cells were incubated in normoxic or hypoxic conditions.

Cell Proliferation and Migration Assay

Cell proliferation was measured using Cell Counting Kit-8 assay (MedChemExpress, MCE, HY-K0301, Monmouth Junction, NJ) with absorbance at 450 nm is proportional to the number of living cells. Cells were initially grown on 96-well plates (1.5 \times 10⁴ cells per well). EdU (5-ethynyl-2'-deoxyuridine)-incorporation assays also were performed to determine HPASMCs proliferation using kFluor488-EdU proliferation detection kit (KeyGEN, KGA331-1000, Nanjing, China). Briefly, HPASMCs were seeded in 24 well plates and were synchronized over 24 hours under serum-free media. HPASMCs were then incubated with complete medium containing 1 μ M 4-HNE, 20 μ M Alda-1, or 60 μ M daidzin for 48 hours under normoxia or hypoxia conditions. The cells were labeled with EdU according to the manufacturer's instructions. The results were acquired using Olympus cellSens imaging software (Olympus, BX43, Tokyo, Japan). Quantification of EdU+ cells was accomplished using the cell counter plugin from the Image J software (National Institutes of Health). The percentage of EdU+ in each field was recorded and analyzed. For time-lapse imaging of HPASMCs migration, HPASMCs were seeded into Culture-Insert 2 Well in μ -Dish 35mm, high (IBIDI, 81176, Martinsried, Germany) in a concentration of 8 \times 10⁴ cells/mL. After the cells form a confluent layer within 2 to 3 days, the μ -Dish was removed and fresh culture medium was added. Then the culture dishes were placed in normoxic and hypoxic conditions. Migration was recorded after 24 hours incubation using Olympus cellSens imaging software (Olympus, BX43, Tokyo, Japan). The number of cells migrating out of the wound edge was scored using Image Pro Plus image analysis software.

Mitochondrial Superoxide Assay

The production of mitochondrial superoxide was measured using a MitoSox Red Mitochondrial Superoxide Indicator (Invitrogen, Eugene, OR). Cells were incubated with 5 μ mol/L MitoSox reagent working solution for 10 minutes at 37°C in

the dark. After washing, cells were pictured with a fluorescent microscope (Olympus, BX43, Tokyo, Japan).

Western Blotting

Lung tissues and cells were sonicated in RIPA (radio immunoprecipitation assay) lysis buffer. Protein concentration was detected by BCA (bicinchoninic acid) assay. Twenty micrograms of protein was separated by 12% SDS-PAGE, then transferred to polyvinylidene difluoride (PVDF) membranes (Merck Millipore, Billerica, MA). After blocking with 5% skim milk in Tris-buffered saline containing 0.1% Tween 20 for an hour at room temperature, the membranes were incubated overnight at 4°C with primary antibodies. After washing, secondary antibodies were incubated for 1 hour. The relative intensity of immunoreactive bands was assessed by Image J software. The results were normalized to β -actin levels and expressed as % of control. All experiments were repeated at least 3 \times .

mRNA Extraction and Sequencing

Total RNA was extracted from lung tissues using TRIzol reagent (Invitrogen) following the manufacturer's instructions and treated with DNase I. RNA purity was checked using the kaiaok5500 Spectrophotometer (Kaiao, Beijing, China). RNA integrity and concentration was assessed using the RNA Nano 6000 Assay Kit of the Bioanalyzer 2100 system (Agilent Technologies, CA). Sequencing libraries were generated using NEBNext Ultra RNA Library Prep Kit for Illumina (no. E7530L, NEB) following the manufacturer's recommendations. RNA Sequencing data analysis was performed by Annoroad Gene Technology Corporation (Beijing, China).

Reverse Transcription Quantitative Polymerase Chain Reaction

To determine the mRNA levels of ALDH2 in lung tissues, total RNA was extracted with TRIzol (Invitrogen Life Technologies, Carlsbad, CA) according to the manufacturer's instructions. Two micrograms of total RNA were reverse-transcribed to cDNA. ABI 7500 quantitative polymerase chain reaction instrument (Applied Biosystems; Thermo Fisher Scientific, Waltham, MA) was used for the real-time polymerase chain reaction analysis.

Detection of ROS

In situ dihydroethidium fluorescence staining were used to assess the production of ROS in lung tissues and HPASMCs. The lung tissues were embedded in optimal cutting temperature compound and cut into 5 μ m cryosections. After washing with PBS, the sections were incubated with dihydroethidium solution (5 μ mol/L; Beyotime Biotechnology, S0063, Nanjing, China) in a light-protected humidified chamber at 37°C for 30 minutes. For cultured HPASMCs, cells were washed with medium and incubated with dihydroethidium (5 μ mol/L) at 37°C for 30 minutes. After rinsing, the slides and cells were imaged with a fluorescence microscope (Olympus, BX43, Tokyo, Japan).

Immunohistochemistry

Lungs were initially perfused with saline through the right ventricle. Then lung tissues were fixed with 4% paraformaldehyde for 24 hours. After dehydration and embedding, the lungs were

cut into 5 μ m sections. Lung tissue sections then were deparaffinized and rehydrated. Endogenous peroxidase was eliminated by 3% H₂O₂. Immunohistochemical assessment of muscularization was performed by staining for rabbit polyclonal anti-alpha smooth muscle Actin antibody (1:100, ab5694; Abcam, Cambridge, MA). Thirty to 40 pulmonary arteries (external diameter of 25–100 μ m) were analyzed according to α -SMA (smooth muscle actin) staining percentages of vessel circumference.²¹ Sections were photographed and assessed by 2 investigators in a blinded fashion.

Viral Vectors

Adeno-associated virus-2 vectors were recombined with enzyme cutting method to carry SM22 α (smooth muscle 22 alpha) promoter, GFP (green fluorescent protein), or ALDH2 coding sequence.²² Adeno-associated virus-1 vectors were recombined to carry ICAM (intercellular adhesion molecule) 2 promoter, GFP, or ALDH2 coding sequence.²³ All virus vectors were designed and constructed by Vigene Biosciences (Rockville, MD).

Immunofluorescence and Confocal Microscopy

Cryosections of lung tissues were incubated with the primary antibodies to evaluate the levels of 4-HNE, malondialdehyde, and ALDH2 in pulmonary arteries indicated by costaining of α SMA. Images were acquired using a fluorescence microscope (Olympus, BX43, Tokyo, Japan) and were analyzed using Image Pro Plus software. To determine mitochondrial fission, HPASMCs were cultured on coverslips (WHB-24-CS-10; WHB Scientific, Shanghai, China) and exposed to different treatments. After removing the media from the dish and prewarmed staining solutions containing MitoTracker probe (ThermoFisher Scientific, M7512, Waltham, MA) were incubated for 30 minutes. The cells were washed with PBS and then were fixed with 4% formaldehyde for 15 minutes. After rinsing several times, cells were costained with DAPI (4',6'-diamidino-2-phenylindole; ab104139, Abcam; Cambridge, MA) for 5 minutes. Images of cells were taken under the confocal laser scanning fluorescence microscopy (LSM710; Carl Zeiss AG, Jena, Germany). Mitochondrial fragmentation versus connectivity was evaluated by plotting length \times width of thousands of mitochondria from >10 cells.²⁴

Statistical Analysis

All the experiments were repeated at least 5 \times . All values are expressed as the mean \pm SEM. Data have passed normality or equal variance tests. Comparisons between groups were performed by Student *t* test or 1-way ANOVA followed by Tukey post hoc test. Transgenic or knockout mouse results were analyzed by 2-way ANOVA, followed by a Bonferroni test. Statistical significance was considered at $P < 0.05$. All data were analyzed using GraphPad Prism version 6.0.

RESULTS

Chronic Hypoxia Increases the Production of 4-HNE

Exposure to chronic hypoxia (3 weeks) increased RVSP, induced RVH, and promoted pulmonary vascular muscularization in C57BL/6 mice (Figure 1 in the [online-only](#)

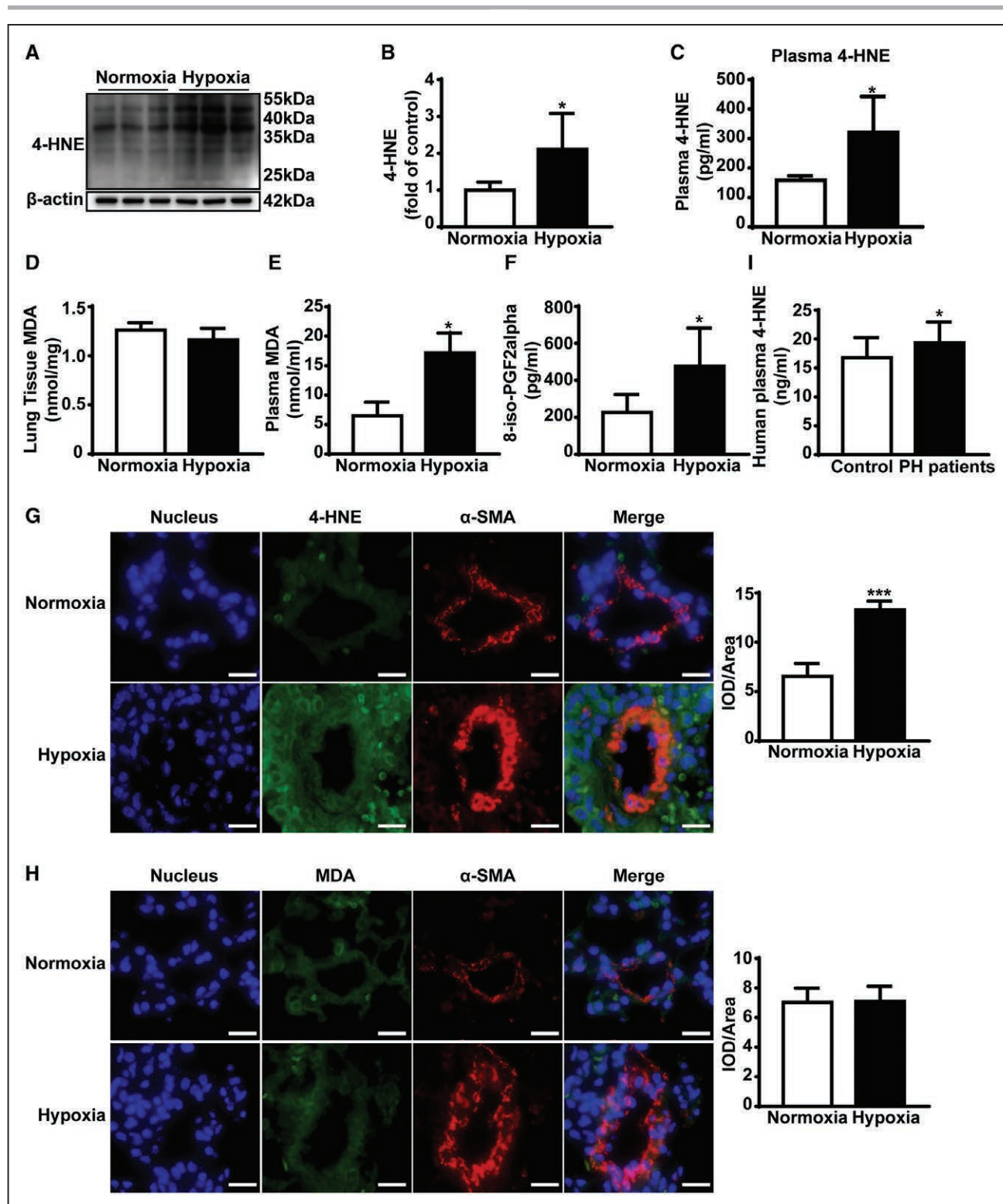


Figure 1. Lipid peroxidation is increased in hypoxia-induced pulmonary arterial hypertension.

A and **B**, Immunoblotting indicated 4-hydroxynonenal (4-HNE) expression in the lung tissues, and relative quantification was analyzed. **C**, Plasma 4-HNE levels were determined by ELISA (n=5). **D** and **E**, Lung tissue malondialdehyde and plasma malondialdehyde were determined by TBA (thiobarbituric acid) method (n=5). **F**, Plasma 8-iso-prostaglandin F2 alpha (8-iso-PGF2α) was assessed by ELISA (n=5). **G**, Representative immunofluorescence images of lung sections stained with anti-4-HNE antibodies (green) and anti-α-SMA (smooth muscle actin) antibodies (red) under normoxia or hypoxia conditions. Cell nuclei were stained with DAPI (4',6-diamidino-2-phenylindole; blue; n=6). Scale bar=20 μm. **H**, Representative immunofluorescence images of lung sections stained with anti-malondialdehyde antibodies (green) and anti-α-SMA antibodies (red) under normoxia or hypoxia. Cell nuclei were stained with DAPI (blue; n=6). Scale bar=20 μm. *P<0.05, **P<0.01 vs normoxic group. **I**, 4-HNE levels were detected by ELISA in plasma from pulmonary hypertension (PH) patients (n=23) and controls (n=19). *P<0.05 vs controls. IOD indicates integrated optical density.

Data Supplement). To evaluate lipid peroxidation in HPH, levels of 4-HNE, malondialdehyde, and 8-iso-PGF2 α were examined. 4-HNE level was significantly increased in both lung tissues and plasma of hypoxic mice compared with that in control mice (Figure 1A, 1B, and 1C). However, chronic hypoxia did not change the production of 4-HNE in hearts, livers, and aortas (Figure IIA, IIB, and IIC in the [online-only Data Supplement](#)). Although a higher level of malondialdehyde was detected in the plasma of HPH mice, no differences were found in malondialdehyde levels in lung, heart, liver, and aorta tissues between the 2 groups (Figure 1D and 1E, Figure IID through IIF in the [online-only Data Supplement](#)). Plasma 8-iso-PGF2 α also was increased in hypoxic mice (Figure 1F). These results indicated that lipid peroxidation was increased in HPH mice. Further immunostaining studies confirmed that 4-HNE but not malondialdehyde was markedly increased in pulmonary arteries in response to hypoxia (Figure 1G and 1H). As lipid peroxidation is increased in PH patients,²⁵ we also tested the plasma levels of 4-HNE in patients and found higher levels of 4-HNE in plasma from PH patients compared with that in controls (Figure 1I).

As one of the major end products of lipid peroxidation, 4-HNE is positively correlated with oxidative stress.²⁶ The levels of ROS then were determined and expectedly, chronic hypoxia increased ROS production in lung tissues (Figure IIIA in the [online-only Data Supplement](#)). To test whether LOs (lipoxygenases) play a role in the production of 4-HNE, we detected the expression of 5-LO, 12-LO, and 15-LO. Expression of all 3 LOs were increased in lung tissues of HPH mice (Figure IIIB through IIIE in the [online-only Data Supplement](#)). Because 12-LO and 15-LO contribute to the production of 4-HNE, 4-HNE should also originate from the enzymatic pathway in chronic hypoxic lung tissues.

Expression of ALDH2 Is Downregulated in Lung Tissues From HPH Mice

To explore the changes in enzymes that are related to metabolism of 4-HNE after exposure to chronic hypoxia, we performed microarray analysis using mRNA extracted from lung tissues of HPH mice and control mice. The expression of 74 genes linked to aldehydes metabolism including aldehyde dehydrogenases, alcohol dehydrogenases, aldehyde reductases, AKR, and glutathione-S-transferases were analyzed (Table III in the [online-only Data Supplement](#)).¹⁴ Compared with normoxia, hypoxia decreased the expression of 13 genes including ALDH2 and increased the expression of 9 genes including ALDH1A1 (ALDH family 1 member A1) in lung tissues (Figure 2A). Effect of chronic hypoxia on ALDH2 gene expression in lung tissues was confirmed with quantitative real-time polymerase chain reaction assay (Figure 2B). Immunoblotting showed that protein

expression of ALDH2 in lung tissues of hypoxia mice was about half of that in lung tissues of control mice (Figure 2C). To confirm the effect of hypoxia on ALDH2, a time-course analysis of ALDH2 expression was performed after exposure to hypoxia. No significant changes in ALDH2 expression were found within the first 2 days, but it was gradually reduced from day 3 under hypoxia (Figure 2D). Figure 2E shows that less ALDH2 was visualized in pulmonary arteries in HPH mice. Interestingly, ALDH2 levels in hearts, livers, and aortas did not differ between the 2 groups (Figure IVA through IVC in the [online-only Data Supplement](#)). Furthermore, less ALDH2 was found in pulmonary arteries in PH patients (Figure 2F). HIF-1 α contributes to the process of hypoxic pulmonary vascular remodeling.²⁷ It was confirmed that levels of HIF-1 α were higher in lung tissues of HPH mice than in those of control mice (Figure 2G).

Overexpression of ALDH2 Prevents the Development of HPH

To investigate the role of ALDH2 in HPH, ALDH2-overexpressing mice (ALDH2-Tg) and wild controls were exposed to normoxic or hypoxic atmospheres for 21 days (Figure 3A). No noticeable differences were found in RVSP, RVH, and pulmonary vascular muscularization between ALDH2-Tg mice and wild mice in normoxic conditions (Figure 3B through 3E). Chronic hypoxia increased RVSP, RVH, and pulmonary vascular muscularization in both genotypes. However, compared with wild mice, RVSP, RVH, and pulmonary vascular muscularization were significantly decreased in ALDH2-Tg mice (Figure 3B through 3E). Moreover, ALDH2 activation effectively prevented the development of HPH (Figure V in the [online-only Data Supplement](#)). Further study using Sugen/hypoxia-induced PH model, we also found ALDH2 activation reduced the severity of PH (Figure VI in the [online-only Data Supplement](#)).

Because ALDH2 plays an important role in detoxifying 4-HNE, we detected the level of 4-HNE by immunoblotting. Under normoxic conditions, the level of 4-HNE in lung tissues of ALDH2-Tg mice did not differ from that in wild mice (Figure 3F). As was expected, 4-HNE level was increased in lung tissues of hypoxic wild mice compared with that in normoxic wild mice (Figure 3F). Compared with hypoxic wild mice, the level of 4-HNE was significantly reduced in lung tissues of ALDH2-Tg mice after chronic hypoxia (Figure 3F). Proliferation of PSMCs or pulmonary arterial endothelial cells contributes to vascular remodeling in pulmonary small resistance arteries.²⁸ Proliferating cell nuclear antigen then was analyzed in lung tissues of mice. Overexpression of ALDH2 did not alter proliferating cell nuclear antigen content in lung tissues under normoxic condition but suppressed the increase of PCNA (proliferating cell nuclear antigen) compared

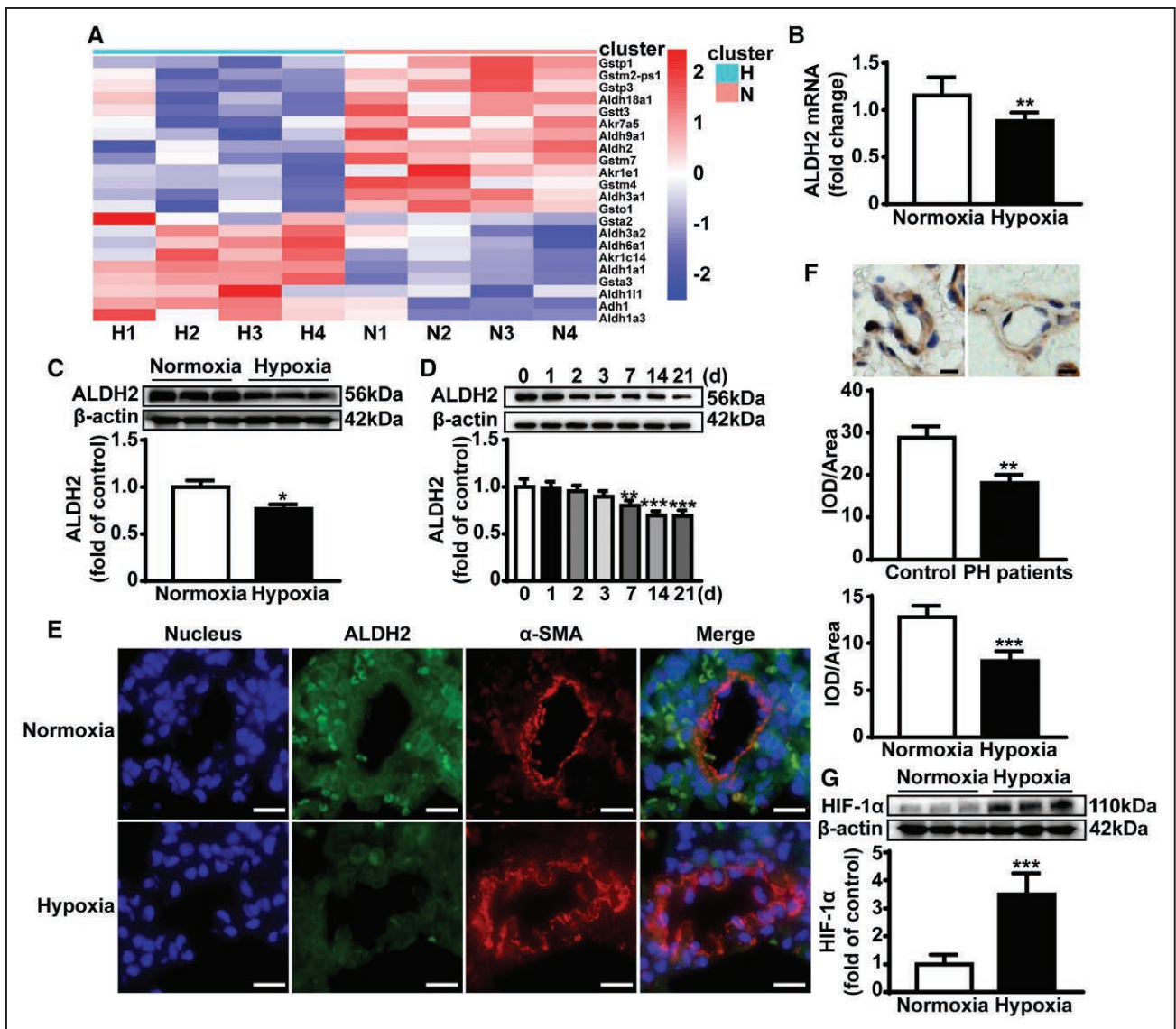


Figure 2. ALDH2 (aldehyde dehydrogenase 2) is decreased by chronic hypoxia in lung tissues and pulmonary arteries.

A, Heat map of the upregulated and downregulated genes which are related to aldehydes metabolism and were analyzed by RNA sequencing. **B**, ALDH2 mRNA expression in lung tissues was tested by quantitative real-time polymerase chain reaction ($n=5$). **C**, Western blot analysis of ALDH2 levels in lung tissues. **D**, Representative western blot showing ALDH2 in lung tissue lysates from mice treated with time gradient of hypoxia ($n=5$). **E**, Representative immunofluorescence images of lung sections stained with anti-ALDH2 antibodies (green) and anti- α -SMA (smooth muscle actin) antibodies (red) under normoxia or hypoxia. Cell nuclei were stained with DAPI (4',6-diamidino-2-phenylindole; blue; $n=6$). Scale bar=20 μ m. **F**, ALDH2 was immunostained in sections of lung tissues from pulmonary hypertension (PH) patients ($n=5$) and controls ($n=5$). Scale bar=10 μ m. **G**, Western blot analysis of HIF (hypoxia-inducible factor)-1 α levels in lung tissues. * $P<0.05$, ** $P<0.01$, *** $P<0.001$ vs normoxic group or controls. H indicates hypoxia group; IOD, integrated optical density; and N, normoxia group.

with that in wild mice under hypoxia (Figure 3G). The level of HIF-1 α was also comparatively analyzed to study the effect of ALDH2 on HIF-1 α in vivo. No differences were found in the level of HIF-1 α between ALDH2-Tg mice and wild mice in normoxic conditions (Figure 3H). Compared with control mice, lower HIF-1 α level was found in lung tissues of ALDH2-Tg mice after chronic hypoxia (Figure 3H). Moreover, the expression of ADH (alcohol dehydrogenase) was also detected and no change of ADH was found in lung tissues exposed to chronic hypoxia and neither was that in ALDH2-Tg or

ALDH2 knockout (ALDH2 $^{-/-}$) mice (Figure IVD and IVE in the [online-only Data Supplement](#)).

Global Knockout of ALDH2 Aggravates HPH

ALDH2 $^{-/-}$ mice and littermate control (ALDH2 $^{+/+}$) mice were used to further determine the effect of ALDH2 on HPH (Figure VIIA in the [online-only Data Supplement](#)). Under normoxia, ALDH2 $^{-/-}$ mice and ALDH2 $^{+/+}$ mice had similar RVSP, RVH, and muscularization of pulmonary vessels (Figure VIIB through VIIE in the [online-only Data](#)

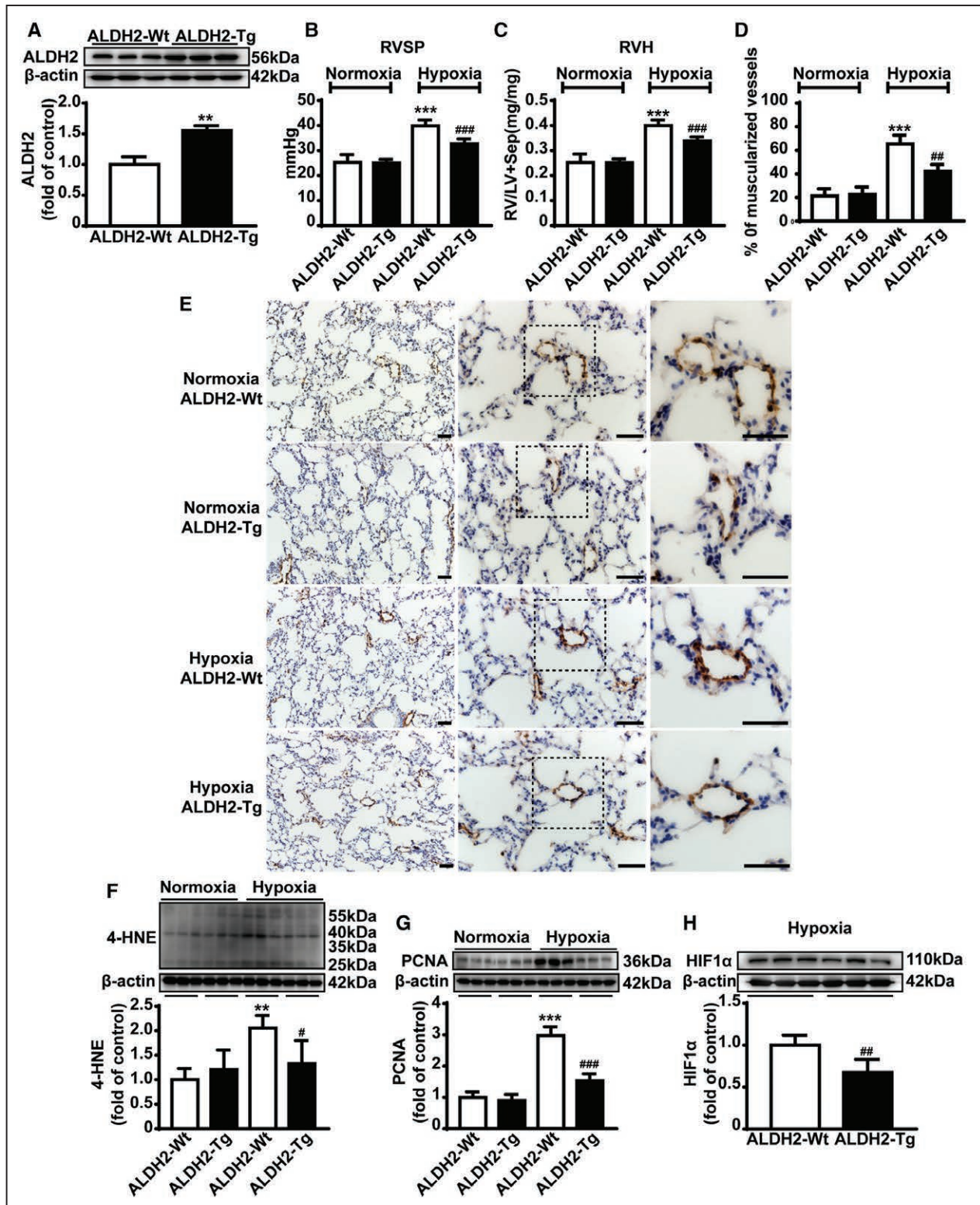


Figure 3. The development of hypoxia-induced pulmonary hypertension (HPH) is attenuated by overexpression of ALDH2 (aldehyde dehydrogenase 2).

A, Western blot analysis of ALDH2 levels in lung tissues from ALDH2 transgenic mice and littermates control. **B** and **C**, Right ventricular systolic pressure (RVSP) and right ventricular hypertrophy (RVH) were measured in ALDH-transgenic (Tg) mice and littermates control exposure to normoxia or hypoxia (n=8). **D**, Percentage of muscularized vessels diameter 25–100 μ m in lung sections (n=8). **E**, Representative sections showing α -SMA (smooth muscle actin) staining. Scale bar=50 μ m. **F** and **G**, Western blot analysis of 4-hydroxynonenal and PCNA (proliferating cell nuclear antigen) in lung tissues. **H**, Western blot analysis of HIF (hypoxia-inducible factor)-1 α levels in lung tissues from ALDH-Tg mice and littermates control under hypoxia. * P <0.05, ** P <0.01, *** P <0.001 vs normoxic ALDH2-wild type (Wt). # P <0.05, ## P <0.01, ### P <0.001 vs hypoxic ALDH2-Wt.

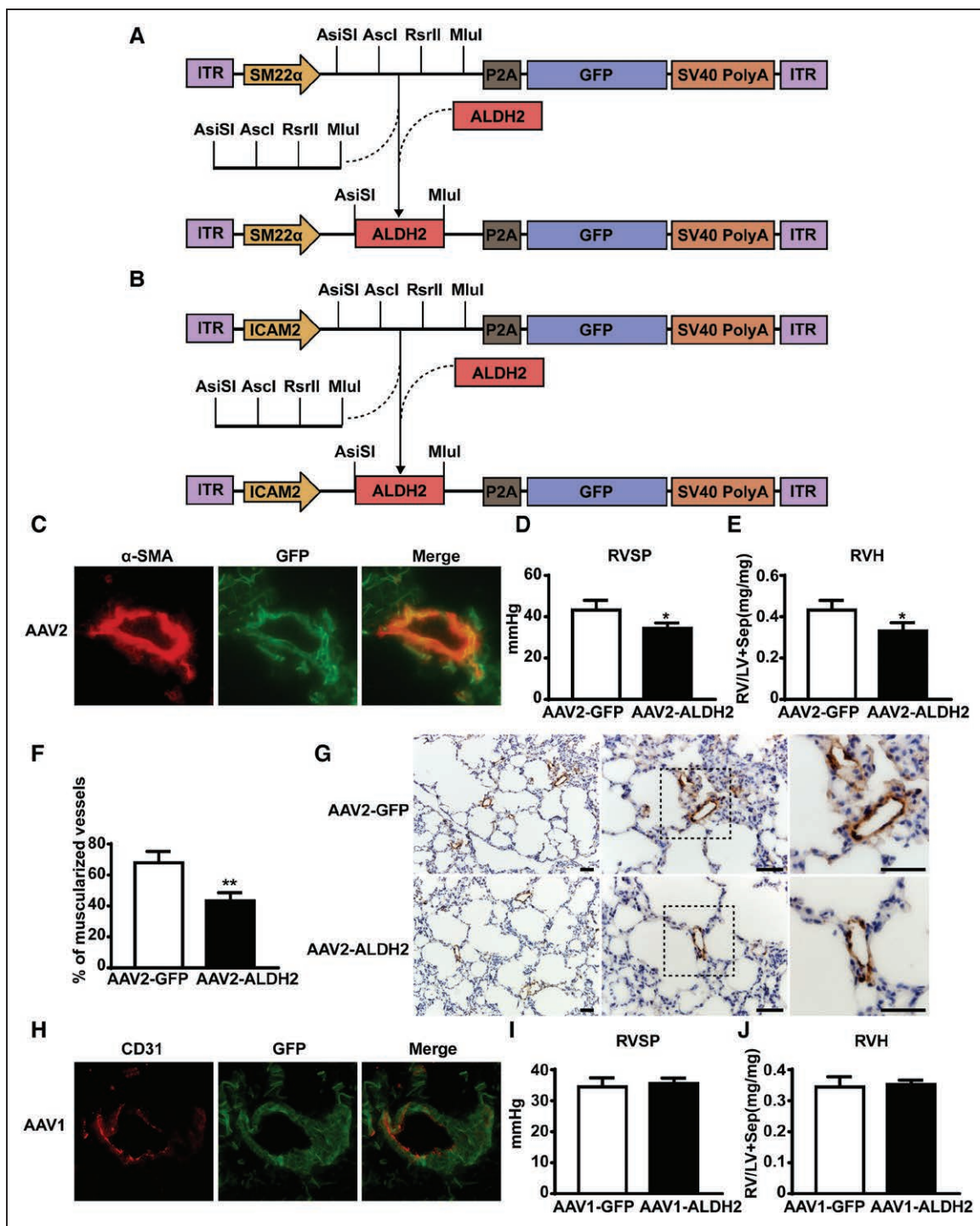


Figure 4. Overexpression of ALDH2 (aldehyde dehydrogenase 2) in pulmonary artery smooth muscle cells prevents the development of HPH.

A and **B**, Vector construction of AAV2 (adeno-associated virus)-SM22α (smooth muscle 22 alpha)-ALDH2 and AAV1-ICAM (intercellular adhesion molecule) 2-ALDH2. **C**, Immunofluorescence location of α-SMA (smooth muscle actin; red) and GFP (green fluorescent protein; green). **D** and **E**, Statistical analysis of right ventricular systolic pressure (RVSP) and right ventricular hypertrophy (RVH) in mice which were treated with AAV2-SM22α-ALDH2 and AAV2-GFP viruses by tail injection (n=7). **F**, Percentage of muscularized vessels diameter 25–100 μm in lung sections (n=7). **G**, Representative sections showing α-SM actin staining. Scale bar=50 μm. **H**, Immunofluorescence location of CD31 (red) and GFP (green). **I** and **J**, Statistical analysis of RVSP and RVH in mice which were treated with AAV1-ICAM2-ALDH2 and AAV1-GFP viruses by tail injection (n=7). *P<0.05, **P<0.01, ***P<0.001 vs control. SV40 indicates Simian virus 40.

Supplement). As expected, chronic hypoxia increased RVSP, RVH, and muscularization of pulmonary vessels in ALDH2^{+/+} mice (Figure VIIIB through VIIE in the [online-only Data Supplement](#)). In contrast to the effect of overexpression of ALDH2 on HPH, ALDH2 deficiency exacerbated the development of HPH as indicated by higher RVSP, RVH, and more muscularization of pulmonary vessels compared with those in control mice (Figure VIIIB through VIIE in the [online-only Data Supplement](#)). ALDH2 deficiency did not change the expression of 4-HNE, PCNA, and HIF-1 α under normoxic conditions, whereas the levels of all were increased under chronic hypoxia compared with those in control mice (Figure VIIF through VIIH in the [online-only Data Supplement](#)).

ALDH2 in PSMCs but not in Pulmonary Arterial Endothelial Cells Contributes to HPH

Both PSMCs and pulmonary arterial endothelial cells play important roles in the development of HPH.^{28,29} To find out through which cell type ALDH2 exerts its effects on HPH, we constructed adeno-associated virus vectors which specifically overexpressed ALDH2 in smooth muscle cells and endothelial cells (Figure 4A and 4B). After [tail vein](#) injection into wide-type mice, strong GFP fluorescence signals were found in PSMCs or pulmonary arterial endothelial cells indicating that the introduction of viruses was successful (Figure 4C and 4H). Compared with AAV2 (adeno-associated virus)-GFP mice, RVSP, RVH, and muscularization of pulmonary vessels were significantly decreased in AAV2-ALDH2 mice (Figure 4D through 4G). However, there were no differences in RVSP and RVH between AAV1-GFP and AAV1-ALDH2 mice (Figure 4I and 4J). Therefore, ALDH2 appears to play an important role in HPH through smooth muscle cells but not endothelial cells.

NAC Attenuates the Severity of HPH in ALDH2^{-/-} Mice

The effect of exogenous NAC on the development of HPH was investigated to determine if ALDH2 protects against HPH via metabolizing 4-HNE. Compared with controls, mice treated with NAC showed a lower RVSP, reduced RVH, and less muscularization of pulmonary vessels (Figure VIIIA through VIIID in the [online-only Data Supplement](#)). The levels of 4-HNE and HIF-1 α were lower in NAC treated hypoxic mice (Figure VIIIE and VIIF in the [online-only Data Supplement](#)). The role of NAC then was tested in ALDH2^{-/-} mice, and NAC treatment decreased RVSP and RVH indicating that severity of HPH was decreased by NAC in ALDH2^{-/-} mice (Figure VIIIG and VIIH in the [online-only Data Supplement](#)). We also determined the direct effect of exogenous 4-HNE on HPH. First, C57BL/6 mice were continuously infused with 4-HNE (0.19 mg/kg per hour, the maximal dose with

an osmotic pump) and were kept in hypoxia for 21 days. Unexpectedly, exogenous 4-HNE failed to change RVSP, RVH, and muscularization of pulmonary vessels compared with those in control mice (Figure IXA, IXB, and IXC in the [online-only Data Supplement](#)). Further study indicated that both plasma levels of 4-HNE and 4-HNE in lung tissues did not differ between the 2 groups (Figure IXD and IXE in the [online-only Data Supplement](#)). Next, we treated mice with a daily peritoneal injection of 4-HNE (10 mg/kg) but still failed to find any differences in RVSP, RVH, and muscularization of pulmonary vessels (data not shown).

ALDH2 Activation Prevents Hypoxia or 4-HNE Induced Proliferation in HPASMCs

The proliferation of HPASMCs was promoted by hypoxia (Figure 5A). To demonstrate the role of ALDH2 in PSMCs proliferation, HPASMCs were incubated with ALDH2 activator and inhibitor under normoxia or hypoxia. Although the proliferation of HPASMCs was not affected by ALDH2 activation or inhibition compared with that in controls under normoxia, ALDH2 activation or inhibition respectively suppressed or promoted HPASMCs proliferation under hypoxia (Figure 5B through 5D). Hypoxia increased the production of 4-HNE but decreased ALDH2 expression in HPASMCs (Figure 5E through 5G). We then overexpressed ALDH2 with adenovirus vectors and found that ALDH2 overexpression also attenuated the effect of hypoxia on HPASMCs proliferation (Figure X in the [online-only Data Supplement](#)). In addition, cell migration was also relieved by ALDH2 activation in hypoxic HPASMCs (Figure XI in the [online-only Data Supplement](#)). As ALDH2 activation prevented hypoxia-induced elevation of 4-HNE while ALDH2 inhibition increased the production of 4-HNE in hypoxic HPASMCs (Figure 5H), exogenous 4-HNE was used to investigate the role of 4-HNE in the proliferation of HPASMCs. 4-HNE promoted the proliferation of HPASMCs in a concentration-dependent manner (Figure 5I). Furthermore, ALDH2 activation attenuated, whereas ALDH2 inhibition enhanced the effect of 4-HNE on the proliferation of HPASMCs (Figure 5J through 5L). Moreover, we found 4-HNE increased intracellular ROS and mitochondrial superoxide production in HPASMCs (Figure XII in the [online-only Data Supplement](#)). Using HPASMCs harvested from PH patients, we confirmed that ALDH2 activation prevented hypoxia or 4-HNE-induced cell proliferation (Figure XIII A through XIII D in the [online-only Data Supplement](#)) and decreased 4-HNE under hypoxia (Figure XIII E through XIII H in the [online-only Data Supplement](#)).

ALDH2 Regulates Hypoxia or 4-HNE Induced Mitochondrial Fission

Mitochondrial fission contributes to hypoxia-induced PSMCs hyperproliferation.³⁰ To reveal the underlying

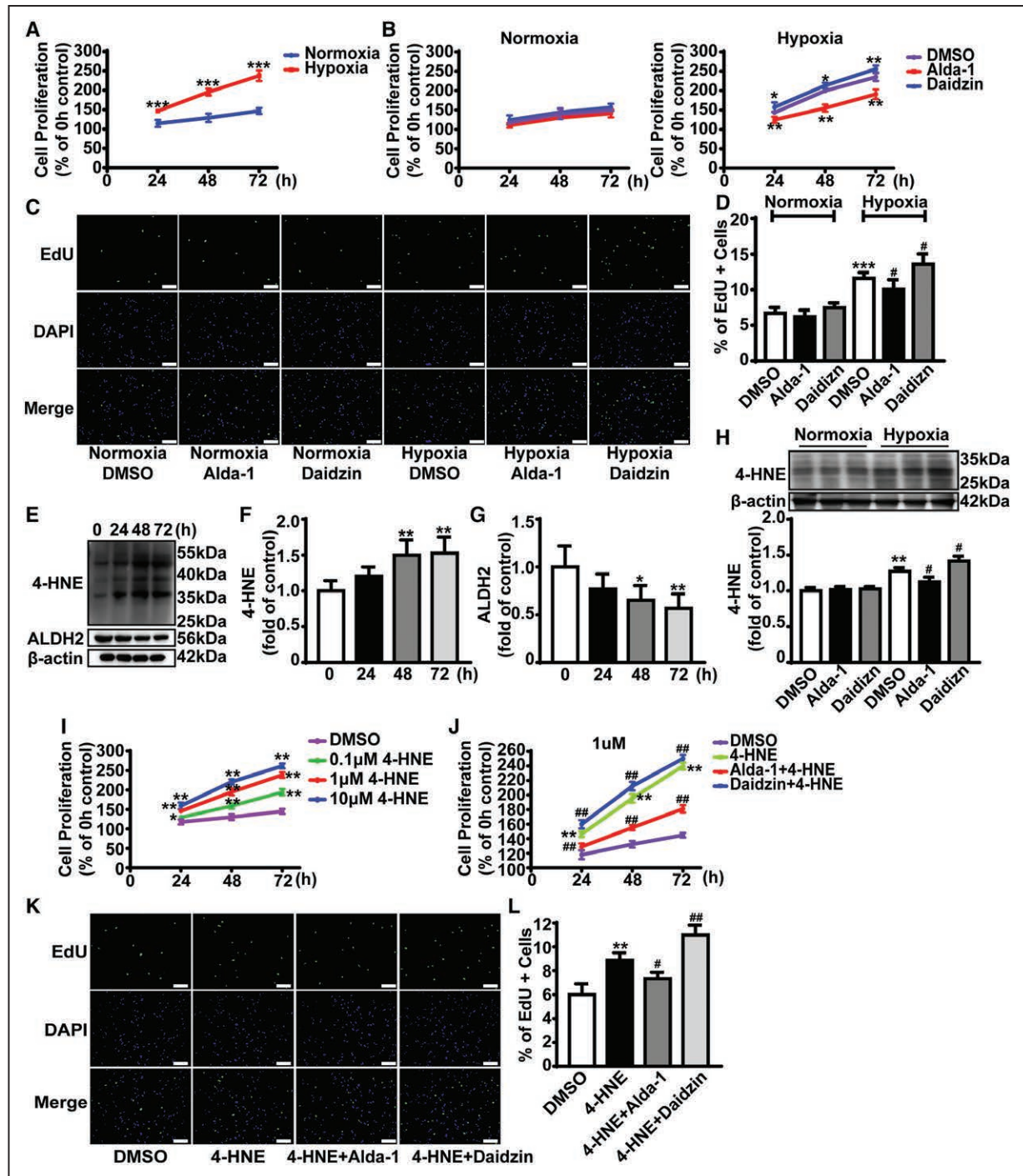


Figure 5. ALDH2 (aldehyde dehydrogenase 2) activation prevents hypoxia or 4-hydroxynonenal (4-HNE)-induced proliferation in human pulmonary artery smooth muscle cells (HPASMCs).

A, The effect of normoxia or hypoxia on HPASMC proliferation, as determined by Cell Counting Kit-8 (CCK8) assays ($n=5$). $***P<0.001$ vs normoxia group. **B**, The effect of Alda-1 or Daidzin on HPASMC proliferation under normoxia or hypoxia was determined by CCK8 assays ($n=5$). $*P<0.05$, $**P<0.01$ vs hypoxia + dimethyl sulfoxide (DMSO) group. **C**, The effect of Alda-1 and Daidzin treatment under hypoxia for 48 h on HPASMCs proliferation was evaluated by EdU (5-ethynyl-2'-deoxyuridine) assays. Scale bar=100 μ m. **D**, Bar graph showing the percentage of EdU incorporated HPASMCs from **C** ($n=5$). $***P<0.001$ vs DMSO group, $\#P<0.05$ vs hypoxia + DMSO group. **E**, Representative blots of 4-HNE and ALDH2 expression in HPASMCs under time gradients of hypoxia. **F** and **G**, Quantification of protein levels from **E**, relative to the control ($n=5$). $*P<0.05$, $**P<0.01$ vs control. **H**, Western blot analysis of 4-HNE levels in HPASMCs stimulated by DMSO, Alda-1, and Daidzin under normoxia or hypoxia ($n=5$). $**P<0.01$ vs DMSO group, $\#P<0.05$ vs hypoxia + DMSO group. **I**, The effect of different concentrations of 4-HNE (0.1, 1, and 10 μ M) on HPASMC proliferation, as determined by CCK8 assays ($n=5$). $**P<0.01$ vs DMSO group. **J**, The effect of Alda-1 or Daidzin on HPASMC proliferation, as determined by CCK8 assays ($n=5$). $**P<0.01$ vs DMSO group, $\#\#P<0.01$ vs 4-HNE group. **K**, The effect of Alda-1 or Daidzin on HPASMC proliferation was evaluated by EdU assays. Scale bar=100 μ m. **L**, Bar graph showing the percentage of EdU incorporated HPASMCs from **K** ($n=5$). $**P<0.01$ vs DMSO group, $\#P<0.05$ vs 4-HNE group.

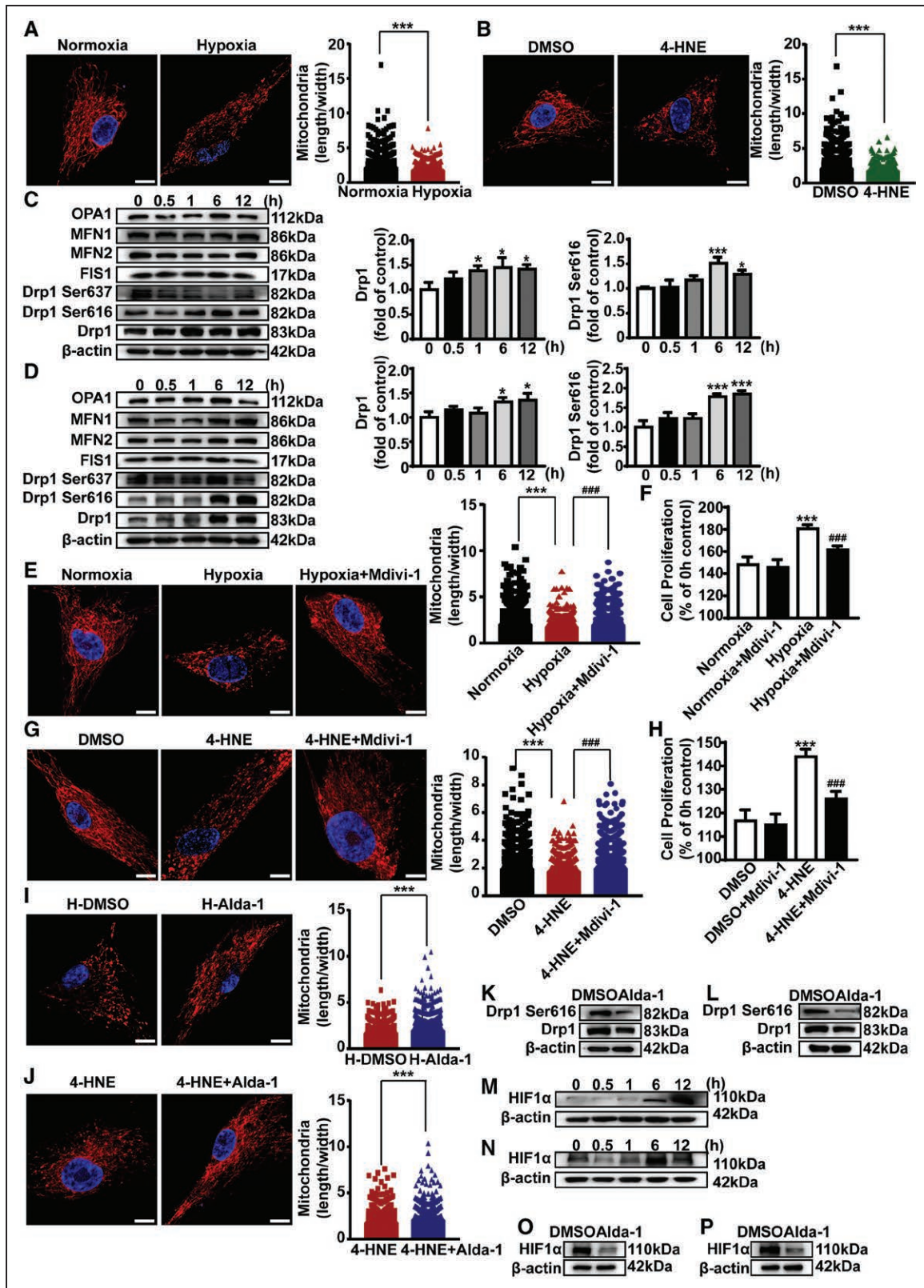


Figure 6. Hypoxia or 4-hydroxynonenal (4-HNE)-induced mitochondrial fission is regulated by ALDH2 (aldehyde dehydrogenase 2). **A** and **B**, Human pulmonary artery smooth muscle cell (HPASMCs) were treated by hypoxia or 4-HNE (1 μM) and were stained with Mitotracker Red and DAPI (4',6-diamidino-2-phenylindole). Mitochondrial morphology was imaged with the confocal laser scanning fluorescence microscopy. Mitochondrial fission was evaluated by the ration of mitochondrial length and width which was plotted for thousands of mitochondria from >10 cells. Scale bar=20 μm. ****P*<0.001 vs normoxia or dimethyl sulfoxide (DMSO) group. **C** and **D**, Western blot analysis of OPA1 (optic atrophy protein 1), MFN (mitofusin) 1, MFN2, FIS1 (mitochondrial fission protein 1), Drp1 (dynamin-related protein 1), phosphorylation of Drp1 (*Continued*)

mechanism through which ALDH2 exerts its effects on HPASMCs proliferation, we then tested the effect of hypoxia and 4-HNE on mitochondrial fission. Compared with controls, hypoxia or 4-HNE significantly increased mitochondrial fission in HPASMCs (Figure 6A and 6B). Next, we determined proteins related to mitochondrial fission and fusion under hypoxia or 4-HNE. No changes were found in the protein levels of OPA1 (optic atrophy protein 1), MFN (mitofusin) 1, MFN2, and Fis1 (mitochondrial fission protein 1) in hypoxic HPASMCs compared with those in normoxic HPASMCs (Figure 6C). 4-HNE stimulation did not change the protein expression of OPA1, MFN1, MFN2, and Fis1 (Figure 6D). Interestingly, both hypoxia and 4-HNE treatment increased the protein level of Drp1 (dynamin-related protein 1; Figure 6C and 6D). Activated Drp1, mediated by phosphorylation at serine 616, moves from the cytosol to the mitochondria and promotes mitochondrial fission, whereas phosphorylation of Drp1 at serine 637 inhibits mitochondrial fission.^{31,32} Hypoxia or 4-HNE increased the phosphorylation of Drp1 at serine 616 but not serine 637 (Figure 6C and 6D). With the inhibitor-Mdivi-1 (mitochondrial division inhibitor), mitochondrial fission was suppressed by Drp1 inhibition in hypoxia or 4-HNE treated HPASMCs (Figure 6E and 6G). More importantly, Drp1 inhibition prevented the effect of hypoxia or 4-HNE on the proliferation of HPASMCs (Figure 6F and 6H). To investigate whether ALDH2 regulates HPASMCs proliferation through mitochondrial fission, we then pretreated HPASMCs with Alda-1 before exposure to hypoxia or 4-HNE. Mitochondrial fission was prevented by ALDH2 activation in hypoxic or 4-HNE-treated HPASMCs compared with that in controls (Figure 6I and 6J). ALDH2 activation decreased the protein level of Drp1 in hypoxic and 4-HNE treated HPASMCs (Figure 6K and 6L). Additionally, HIF-1 α activation induces cyclin B1/CDK1 (cyclin-dependent kinase 1)-dependent phosphorylation of Drp1 at serine 616.³⁰ Expectedly, both hypoxia and 4-HNE increased the stabilization of HIF-1 α (Figure 6M and 6N). ALDH2 activation decreased the level of HIF-1 α in hypoxia-treated or 4-HNE-treated HPASMCs (Figure 6O and 6P). The effect of hypoxia and 4-HNE on HIF-1 α might be mediated by increased phosphorylation of P38 MAPK (mitogen-activated protein kinase; Figure XIVA and XIVB in the [online-only Data Supplement](#)). On further study with a HIF-1 α inhibitor, it was confirmed that HIF-1 α contributed to hypoxia and 4-HNE induced mitochondrial fission

(Figure XIVC and XIVD in the [online-only Data Supplement](#)) and HPASMCs proliferation (Figure XIVE and XIVF in the [online-only Data Supplement](#)). Phosphorylation of Drp1 at serine 616 induced by hypoxia or 4-HNE was regulated by HIF-1 α (Figure XIVG and XIVH in the [online-only Data Supplement](#)). To confirm the effect of ALDH2 activation on mitochondrial fission, HPASMCs harvested from PH patients were used. Similarly, hypoxia or 4-HNE treatment induced mitochondria fission, increased Drp1 expression, and promoted the phosphorylation of Drp1 at serine 616 in HPASMCs from PH patients (Figure XVA through XVD in the [online-only Data Supplement](#)). More importantly, it was confirmed that ALDH2 activation decreased hypoxia or 4-HNE-induced mitochondrial fission accompanied with lower levels of Drp1, phosphorylation of Drp1 at serine 616, and HIF-1 α (Figure XVE through XVL in the [online-only Data Supplement](#)).

DISCUSSION

In this study, levels of 4-HNE but not malondialdehyde increased in lung tissues after chronic exposure to hypoxia. Elevated 4-HNE level might be associated with excessive ROS generation and increased expression of LOs. Overexpression of ALDH2 decreased the level of 4-HNE and alleviated the severity of HPH, whereas reverse effects were seen in ALDH2 knockout mice. Using tissue-specific overexpression of ALDH2 virus vectors, ALDH2 in SMCs was found to be more important than that in endothelial cells for the development of HPH. ALDH2 activation prevents hypoxia or 4-HNE induced mitochondrial fission and proliferation of HPASMCs possibly via stabilization of HIF-1 α and phosphorylation of Drp1 at serine 616 as critical molecular pathways (Figure 7). These findings provide new insights into the critical role of lipid peroxidation in HPH and suggesting ALDH2 as a potential therapeutic target by detoxifying 4-HNE.

Lipid peroxidation is increased in patients with PH.^{25,33} Generally, lipid peroxidation is mediated by 3 distinct pathways, namely enzymatic, free radical, and nonenzymatic, nonradical pathways.³⁴ LOs, cyclooxygenases, and cytochrome P450 monooxygenases are the major participants in the enzymatic pathway.³⁵ Lipids also are oxidized directly by oxidative stress. Nonenzymatic, nonradical-dependent lipid peroxidation is mainly mediated by singlet oxygen and ozone.³⁶ Increased ROS are mainly produced by mitochondria and NOX, such as NOX4, in hypoxic

Figure 6 Continued. at serine (Ser)616 and Ser637 levels in HPASMCs under various time periods of hypoxia or 4-HNE stimulation. Relative expressions of Drp1 and Drp1 Ser616 were quantitatively analyzed (n=5). * P <0.05, *** P <0.001 vs normoxia or DMSO group at 0 h. **E** and **G**, Role of the Drp1 inhibitor Mdivi-1 (mitochondrial division inhibitor; 25 μ M) in hypoxia or 4-HNE induced mitochondrial fission. Scale bar=20 μ m. *** P <0.001 vs normoxia or DMSO group, ### P <0.001 vs hypoxia or 4-HNE group. **F** and **H**, The effect of Mdivi-1 on hypoxia or 4-HNE induced HPASMCs proliferation, as determined by CCK8 assays (n=5). *** P <0.001 vs normoxia or DMSO group, ### P <0.001 vs hypoxia or 4-HNE group. **I** and **J**, Effect of ALDH2 activation on mitochondrial fission. Scale bar=20 μ m. *** P <0.001 vs hypoxia or 4-HNE group. **K** and **L**, Representative western blot of Drp1 and Drp1 ser616 in HPASMCs, which is stimulated by Alda-1 under hypoxia or 4-HNE stimulation (n=5). **M** and **N**, Representative western blot of HIF (hypoxia-inducible factor)-1 α under time gradients of hypoxia or 4-HNE (n=5). **O** and **P**, Representative western blot indicated the effect of Alda-1 on HIF-1 α in hypoxic or 4-HNE treated HPASMCs (n=5).

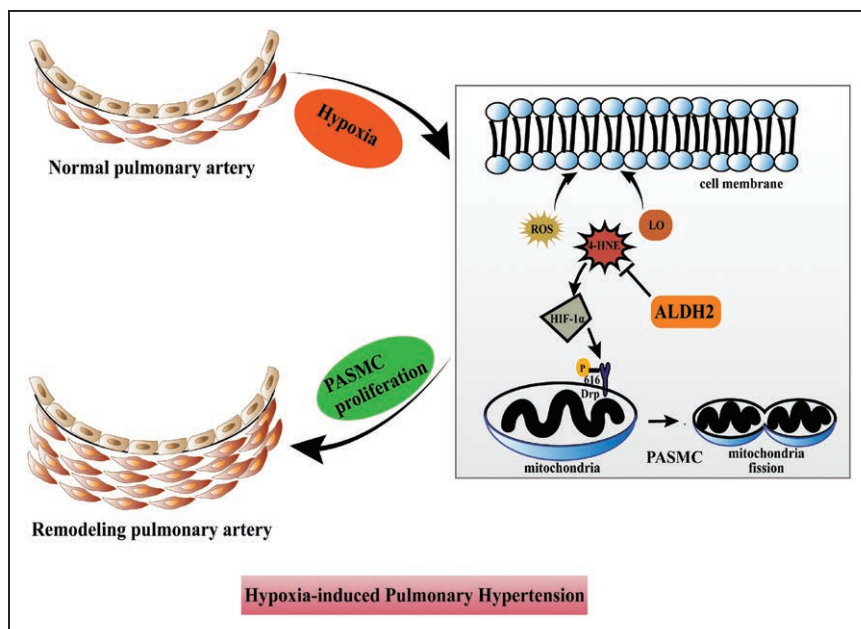


Figure 7. A model of protective effects of ALDH2 (aldehyde dehydrogenase 2) in hypoxia-induced pulmonary hypertension.

4-HNE indicates 4-hydroxynonenal; Drp1, dynamin-related protein 1; HIF, hypoxia-inducible factor; LO, lipoxygenase; PASM, pulmonary artery smooth muscle cell; and ROS, reactive oxygen species.

pulmonary vascular cells.^{11,37} The activity or expression of LOs in pulmonary arteries is also increased by exposure to chronic hypoxia.^{13,38} Consistent with previous studies, we found increased ROS generation and expression of LOs (5-LO, 12-LO, and 15-LO) in chronic lung tissues. Moreover, chronic hypoxia increased plasma 8-iso-PGF₂ α which is a maker of nonenzymatic free radical-catalyzed lipid peroxidation. Therefore, lipid peroxidation should be increased through at least 2 pathways—free radical and enzymatic-dependent pathways under chronic hypoxic conditions. A wide variety of oxidation products are produced by lipid peroxidation including hydroxyoctadecadienoic acids, hydroperoxyeicosatetraenoic acids, epoxyeicosatrienoic acids, lipoxins, leukotrienes, hepoxilins, prostaglandins, and toxic aldehydes.¹¹ Among these products, 5-hydroperoxyeicosatetraenoic acid, 12-hydroperoxyeicosatetraenoic acid, 15-hydroperoxyeicosatetraenoic acid, epoxyeicosatrienoic acids, and leukotriene B are involved in the development of HPH by regulating PASM proliferation, inflammation, or endothelial function.¹³ Thus, increased lipid peroxidation should be closely related to HPH through multiple molecular pathways.

We found that plasma levels of 4-HNE and malondialdehyde were both increased after chronic hypoxia but that the level of 4-HNE and not malondialdehyde was markedly increased in hypoxic lung tissues and pulmonary arteries. Both 4-HNE and malondialdehyde are the toxic aldehydes produced by lipid peroxidation via enzymatic processes and nonenzymatic processes.¹¹ Therefore, it defied common sense that malondialdehyde was not elevated in the increased lipid peroxidation setting in hypoxic lung tissues. One possible explanation is the altered expression of metabolizing enzymes in chronic lung tissues because we found that chronic hypoxia reduces ALDH2 but increases ALDH1A1 in lung tissues,

and 4-HNE is detoxified mainly by ALDH2, whereas malondialdehyde is metabolized mostly by ALDH1A1.^{18,39} Interestingly, we found no effect of chronic hypoxia on 4-HNE production in hearts, livers, and aortas indicating that 4-HNE might not be the major participant in chronic hypoxia-related damages on hearts, livers, and aortas.⁴⁰

4-HNE is the major type of 4-hydroxyalkenals end products generated by oxidation of arachidonic acid and polyunsaturated fatty acids.⁴¹ As one of the major end products of lipid peroxidation, 4-HNE was produced in various cells, including endothelial cells, smooth muscle cells,¹¹ and alveolar epithelial cells (Figure XVI in the [online-only Data Supplement](#)). In this study, 4-HNE has protective functions that enhance cellular antioxidant capacity mainly by regulating transcription factors, including Nrf2 (nuclear factor erythroid 2-related factor 2), AP-1 (activating protein 1), NF (nuclear factor)- κ B, and PPAR (peroxisome-proliferator-activated receptors) as a signaling molecule at lower levels.¹¹ At intermediate levels, 4-HNE affects autophagy, senescence, cell cycle, and cell proliferation. However, higher levels of 4-HNE are toxic to cells leading to cell apoptosis or necroptosis because of its extraordinary tendency to react with proteins or nucleic acids, generating various adducts and leading to protein dysfunction and DNA damage.³⁴ 4-HNE is increased in patients with pulmonary arterial hypertension.⁴² In our study, we failed to find the positive effects of exogenous 4-HNE on HPH by means of intraperitoneal injection or subcutaneous implantation with miniosmotic pumps, which might be explained by the fact that exogenous 4-HNE is rapidly metabolized by cells (within 3 minutes).¹⁴ Nevertheless, 4-HNE should play an important role in the development of HPH because the antioxidant-NAC decreases the level of 4-HNE and alleviates pulmonary arterial pressures of HPH mice.

ALDH2, a tetrameric allosteric mitochondrial enzyme, is best known for its critical detoxifying role in ethanol metabolism.⁴³ Because ALDH2 is expressed ubiquitously in all tissues and plays a key role in oxidizing endogenous toxic aldehydes including 4-HNE and malondialdehyde, it has been implicated in several pathologies including cardiovascular diseases, diabetes mellitus, neurological dysfunction, and ischemia-reperfusion injury.⁴³ Recently, activation of ALDH2 was proved to reduce RVSP in a monocrotaline-induced pulmonary arterial hypertension animal model.¹⁹ The present study is to our knowledge, the first report that ALDH2 plays a protective role in HPH as evidenced using ALDH2 transgenic and knockout mice. Interestingly, overexpression of ALDH2 specifically in smooth muscle cells but not endothelial cells was protective against HPH. ALDH2 plays a protective role in many oxidative stress associated diseases including myocardial infarction, myocardial ischemia/reperfusion injury, and stroke by clearing 4-HNE.^{16–18} We also found a decreased content of 4-HNE in lung tissues from ALDH2-overexpressing mice but an increased content of 4-HNE in lung tissues from ALDH2 knockout mice. NAC prevents the development of HPH of ALDH2 knockout mice. Moreover, activation of ALDH2 decreases the level of 4-HNE in HPASMCs. Thus, 4-HNE appears to be the critical downstream signal pathway in the protective role of ALDH2 in HPH. Moreover, ALDH2 activation decreased the serum levels of interleukin-1 β , interleukin-6, and Fizz1 (found in inflammatory zone protein 1) in HPH mice (Figure XVII in the [online-only Data Supplement](#)). Thus, it should be speculated that ALDH2 might also effect on HPH through regulating inflammation and even activation of macrophages which should be explored in the future.

Smooth muscle cell proliferation is a critical contributor to pulmonary arterial remodeling in HPH.^{8,29} Chronic hypoxia leads to proliferation of PSMCs, resulting in significant thickening of the muscular layers and muscularization of nonmuscular arteries *in vivo*.²⁹ Although the effect of hypoxia on PSMCs proliferation remains controversial, a growing number of studies have documented the accelerating effect of hypoxia *in vitro*.²⁸ In the present study, we confirmed that hypoxia promoted HPASMCs proliferation. More importantly, ALDH2 functions as a regulatory molecule in hypoxia-induced smooth muscle cell proliferation as shown by using an ALDH2 agonist and an antagonist. 4-HNE induces HPASMCs proliferation.¹⁹ We also obtained similar results and found that 4-HNE enhanced hypoxia-induced HPASMCs proliferation which was regulated by ALDH2, thereby underscoring that ALDH2 exerts its effects on HPASMCs proliferation via regulating the level of 4-HNE.

Mitochondria normally serve as energy powerhouses and redox sensors in PSMCs.⁴⁴ Mitochondria change their overall morphology and proliferate by their fusion and fission in response to the cellular environment and differentiation.⁴⁵ Mitochondria fusion and fission are

mainly mediated by membrane-remodeling mechanochemical enzymes. MFN1 and MFN2 mediate fusion of the mitochondrial outer membrane, and OPA1 mediates the fusion of the mitochondrial inner membrane, whereas Drp1 and FIS1 are involved in mitochondrial fission.⁴⁵ Increased mitochondrial fission, which is associated with cyclin B-CDK1 and ERK (extracellular signal-regulated kinase)-dependent phosphorylation of Drp1 at serine 616, plays an important role in hypoxia-induced HPASMCs proliferation.^{30,46} Furthermore, MFN1 is involved in hypoxia effects by regulating mitochondrial homeostasis and function.⁴⁷ Hypoxia or 4-HNE treatment increased mitochondrial fission. Elevation of phosphorylation of Drp1 at serine 616 mediates hypoxia-induced mitochondria fission.³⁰ We found that 4-HNE also increased phosphorylation of Drp1 at serine 616. Although it was reported that the expression of MFN1, MFN2, and OPA1 could be changed by hypoxia, we did not find noticeable differences in the expression of these proteins in hypoxic HPASMCs as compared with that in controls.⁴⁷ We also found that 4-HNE treatment had no effect on the expression of MFN1, MFN2, and OPA1. Using a Drp1 inhibitor, we demonstrated that mitochondrial fission contributes to hypoxia or 4-HNE induced HPASMCs proliferation. HIF-1 α activation mediates phosphorylation of Drp1 at serine 616 under hypoxia.⁴⁷ Interestingly, 4-HNE also increases HIF-1 α stabilization which might be mediated by increased phosphorylation of P38 MAPK.⁴⁸ HIF-1 α is regulated by oxygen levels through a dual system of prolyl and asparaginyl hydroxylation. Prolyl hydroxylation mediated by prolyl hydroxylases promotes von Hippel-Lindau ubiquitin E3 ligase-mediated proteasomal degradation of HIF-1 α .⁹ Because 4-HNE treatment induces modification of 20S and 26S proteasomal forms and decreases the proteasomal activity, the association between 4-HNE and HIF-1 α should be further explored in the future.⁴⁹ ALDH2 improves mitochondrial function by maintaining mitochondrial membrane potential and preventing cytochrome c release.^{50,51} However, we found ALDH2 deficient but not ALDH2 overexpressed PSMCs showed increased oxygen consumption rate (Figure XVIII in the [online-only Data Supplement](#)). Thus, the effect of ALDH2 on mitochondrial function remains to be explored.

In summary, the present study demonstrated that increased 4-HNE plays a critical role in the development of HPH by stabilizing HIF-1 α , inducing phosphorylation of Drp1 at serine 616, promoting mitochondrial fission, and subsequently enhancing PSMCs proliferation. As the detoxifying enzyme, ALDH2 in smooth muscle cell plays a major role in preventing HPH, indicating that PSMCs proliferation is a key pathway by which lipid peroxidation exerts its effects on HPH. Furthermore, ALDH2 could be a potential pharmacological target for the therapy of HPH and other lipid peroxidation related diseases.

ARTICLE INFORMATION

Received May 16, 2019; accepted August 28, 2019.

Affiliations

From the Department of Emergency and Chest Pain Center, Qilu Hospital, Shandong University (Y.Z., J.Z., D.H., Q.Z., C.P., Q.Y., F.X., S.W., Y.C.), Clinical Research Center for Emergency and Critical Care Medicine of Shandong Province, Institute of Emergency and Critical Care Medicine of Shandong University, Qilu Hospital, Shandong University (Y.Z., J.Z., D.H., Q.Z., C.P., Q.Y., F.X., S.W., Y.C.), Key Laboratory of Emergency and Critical Care Medicine of Shandong Province, Key Laboratory of Cardiopulmonary-Cerebral Resuscitation Research of Shandong Province, Qilu Hospital, Shandong University (Y.Z., J.Z., D.H., Q.Z., C.P., Q.Y., F.X., S.W., Y.C.), The Key Laboratory of Cardiovascular Remodeling and Function Research, Chinese Ministry of Education, Chinese Ministry of Health and Chinese Academy of Medical Sciences; The State and Shandong Province Joint Key Laboratory of Translational Cardiovascular Medicine, Qilu Hospital, Shandong University (Y.Z., J.Z., D.H., Q.Z., C.P., Q.Y., F.X., S.W., Y.C.), and Clinical Trial Center (B.W.), Qilu Hospital of Shandong University, Jinan; College of Veterinary Medicine, Northwest A&F University, Yangling, Shaanxi, China (Y.S., H.T.); and State Key Laboratory of Respiratory Disease, National Clinical Research Center for Respiratory Disease, Guangdong Key Laboratory of Vascular Disease, Guangzhou Institute of Respiratory Health, The First Affiliated Hospital of Guangzhou Medical University, Guangdong, China (H.T.).

Sources of Funding

This study was supported by the National Key R&D Program of China (2017YFC0908700, 2017YFC0908703), National Natural Science Foundation of China (81772036, 81601717, 81873950, 81570401, 81571934), National S&T Fundamental Resources Investigation Project (2018FY100600, 2018FY100602), Taishan Pandeng Scholar Program of Shandong Province (tspd20181220), Taishan Young Scholar Program of Shandong Province (tsqn20161065, tsqn201812129), Key R&D Program of Shandong Province (2016GSF201235, 2016ZDJS07A14, 2018GSF118003), Shandong Medical and Health Science Technology Development Plan Project (2018WS329), Science Foundation of Qilu Hospital of Shandong University (2015QLQN13), and the Fundamental Research Funds of Shandong University (2018JUC011).

Disclosures

None.

REFERENCES

- Galie N, Humbert M, Vachiery JL, et al. 2015 ESC/ERS guidelines for the diagnosis and treatment of pulmonary hypertension: the joint task force for the diagnosis and treatment of pulmonary hypertension of the European Society of Cardiology (ESC) and the European Respiratory Society (ERS): endorsed by: association for European Paediatric and Congenital Cardiology (AEPC), International Society for Heart and Lung Transplantation (ISHLT). *Eur Heart J*. 2016;37:67–119.
- Nathan SD, Barbera JA, Gaine SP, Harari S, Martinez FJ, Olschewski H, Olsson KM, Peacock AJ, Pepke-Zaba J, Provencher S, et al. Pulmonary hypertension in chronic lung disease and hypoxia. *Eur Respir J*. 2019; 53:1801914.
- Wilkins MR, Ghofrani HA, Weissmann N, Aldashev A, Zhao L. Pathophysiology and treatment of high-altitude pulmonary vascular disease. *Circulation*. 2015;131:582–590.
- Vonk Noordegraaf A, Westerhof BE, Westerhof N. The relationship between the right ventricle and its load in pulmonary hypertension. *J Am Coll Cardiol*. 2017;69:236–243.
- Rowan SC, Keane MP, Gaine S, McLoughlin P. Hypoxic pulmonary hypertension in chronic lung diseases: novel vasoconstrictor pathways. *Lancet Respir Med*. 2016;4:225–236.
- Hoepfer MM, McLaughlin VV, Dalaan AM, Satoh T, Galie N. Treatment of pulmonary hypertension. *Lancet Respir Med*. 2016;4:323–336.
- Tuder RM. Pulmonary vascular remodeling in pulmonary hypertension. *Cell Tissue Res*. 2017;367:643–649.
- Ball MK, Waypa GB, Mungai PT, Nielsen JM, Czech L, Dudley VJ, Beussink L, Dettman RW, Berkelhamer SK, Steinhorn RH, et al. Regulation of hypoxia-induced pulmonary hypertension by vascular smooth muscle hypoxia-inducible factor-1 α . *Am J Respir Crit Care Med*. 2014;189:314–324.
- Bishop T, Ratcliffe PJ. Hif hydroxylase pathways in cardiovascular physiology and medicine. *Circ Res*. 2015;117:65–79.
- Sommer N, Strielkov I, Pak O, Weissmann N. Oxygen sensing and signal transduction in hypoxic pulmonary vasoconstriction. *Eur Respir J*. 2016;47:288–303.
- Ayala A, Munoz MF, Arguelles S. Lipid peroxidation: production, metabolism, and signaling mechanisms of malondialdehyde and 4-hydroxy-2-nonenal. *Oxid Med Cell Longev*. 2014;2014:360438.
- Wei SJ, Xing JH, Wang BL, Xue L, Wang JL, Li R, Qin WD, Wang J, Wang XP, Zhang MX, et al. Poly(ADP-ribose) polymerase inhibition prevents reactive oxygen species induced inhibition of aldehyde dehydrogenase2 activity. *Biochim Biophys Acta*. 2013;1833:479–486.
- Sharma S, Ruffenach G, Umar S, Motayagheni N, Reddy ST, Eghbali M. Role of oxidized lipids in pulmonary arterial hypertension. *Pulm Circ*. 2016;6:261–273.
- O'Brien PJ, Siraki AG, Shangari N. Aldehyde sources, metabolism, molecular toxicity mechanisms, and possible effects on human health. *Crit Rev Toxicol*. 2005;35:609–662.
- Vasilioi V, Nebert DW. Analysis and update of the human aldehyde dehydrogenase (ALDH) gene family. *Hum Genomics*. 2005;2:138–143.
- Ma H, Guo R, Yu L, Zhang Y, Ren J. Aldehyde dehydrogenase 2 (aldh2) rescues myocardial ischaemia/reperfusion injury: role of autophagy paradox and toxic aldehyde. *Eur Heart J*. 2011;32:1025–1038.
- Chen CH, Budas GR, Churchill EN, Disatnik MH, Hurley TD, Mochly-Rosen D. Activation of aldehyde dehydrogenase-2 reduces ischemic damage to the heart. *Science*. 2008;321:1493–1495.
- Guo JM, Liu AJ, Zang P, Dong WZ, Ying L, Wang W, Xu P, Song XR, Cai J, Zhang SQ, et al. ALDH2 protects against stroke by clearing 4-HNE. *Cell Res*. 2013;23:915–930.
- Xu T, Liu S, Ma T, Jia Z, Zhang Z, Wang A. Aldehyde dehydrogenase 2 protects against oxidative stress associated with pulmonary arterial hypertension. *Redox Biol*. 2017;11:286–296.
- Ciucian L, Morneau O, Hussey M, Duggan N, Holmes AM, Good R, Stringer R, Jones P, Morrell NW, Jarai G, et al. A novel murine model of severe pulmonary arterial hypertension. *Am J Respir Crit Care Med*. 2011;184:1171–1182.
- Liu M, Liu Q, Pei Y, et al. Aqp-1 gene knockout attenuates hypoxic pulmonary hypertension of mice. *Arterioscler Thromb Vasc Biol*. 2019;39:48–62.
- Akyurek LM, Yang ZY, Aoki K, San H, Nabel GJ, Parmacek MS, Nabel EG. Sm22 α promoter targets gene expression to vascular smooth muscle cells in vitro and in vivo. *Mol Med*. 2000;6:983–991.
- Velasco B, Ramirez JR, Relloso M, Li C, Kumar S, Lopez-Bote JP, Perez-Barriocanal F, Lopez-Novoa JM, Cowan PJ, d'Apice AJ, et al. Vascular gene transfer driven by endoglin and ICAM-2 endothelial-specific promoters. *Gene Ther*. 2001;8:897–904.
- Anderson GR, Wardell SE, Kahir M, Yip C, Ahn YR, Ali M, Yllanes AP, Chao CA, McDonnell DP, Wood KC. Dysregulation of mitochondrial dynamics proteins are a targetable feature of human tumors. *Nat Commun*. 2018;9:1677.
- Cracowski JL, Cracowski C, Bessard G, Pepin JL, Bessard J, Schwebel C, Stanke-Labesque F, Pison C. Increased lipid peroxidation in patients with pulmonary hypertension. *Am J Respir Crit Care Med*. 2001;164:1038–1042.
- Breitzig M, Bhimineni C, Lockey R, Kolliputi N. 4-hydroxy-2-nonenal: a critical target in oxidative stress? *Am J Physiol Cell Physiol*. 2016;311:C537–C543.
- Shimoda LA, Manalo DJ, Sham JS, Semenza GL, Sylvester JT. Partial HIF-1 α deficiency impairs pulmonary arterial myocyte electrophysiological responses to hypoxia. *Am J Physiol Lung Cell Mol Physiol*. 2001;281:L202–208.
- Pak O, Aldashev A, Welsh D, Peacock A. The effects of hypoxia on the cells of the pulmonary vasculature. *Eur Respir J*. 2007;30:364–372.
- Stenmark KR, Fagan KA, Frid MG. Hypoxia-induced pulmonary vascular remodeling: cellular and molecular mechanisms. *Circ Res*. 2006;99:675–691.
- Marsboom G, Toth PT, Ryan JJ, et al. Dynamin-related protein 1-mediated mitochondrial mitotic fission permits hyperproliferation of vascular smooth muscle cells and offers a novel therapeutic target in pulmonary hypertension. *Circ Res*. 2012;110:1484–1497.
- Hong Z, Kuttly S, Toth PT, Marsboom G, Hammel JM, Chamberlain C, Ryan JJ, Zhang HJ, Sharp WW, Morrow E, et al. Role of dynamin-related protein 1 (drp1)-mediated mitochondrial fission in oxygen sensing and constriction of the ductus arteriosus. *Circ Res*. 2013;112:802–815.
- Schmitt K, Grimm A, Dallmann R, Oettinghaus B, Restelli LM, Witzig M, Ishihara N, Mihara K, Ripberger JA, Albrecht U, et al. Circadian control of drp1 activity regulates mitochondrial dynamics and bioenergetics. *Cell Metab*. 2018;27:657–666.e655.
- Cracowski JL, Degano B, Chabot F, et al. Independent association of urinary f2-isoprostanes with survival in pulmonary arterial hypertension. *Chest*. 2012;142:869–876.

34. Niki E, Yoshida Y, Saito Y, Noguchi N. Lipid peroxidation: mechanisms, inhibition, and biological effects. *Biochem Biophys Res Commun*. 2005;338:668–676.
35. Caro AA, Cederbaum AI. Role of cytochrome p450 in phospholipase a2- and arachidonic acid-mediated cytotoxicity. *Free Radic Biol Med*. 2006;40:364–375.
36. Niki E. Role of vitamin E as a lipid-soluble peroxy radical scavenger: in vitro and in vivo evidence. *Free Radic Biol Med*. 2014;66:3–12.
37. Mittal M, Roth M, Konig P, et al. Hypoxia-dependent regulation of nonphagocytic nadph oxidase subunit nox4 in the pulmonary vasculature. *Circ Res*. 2007;101:258–267.
38. Zhu D, Ran Y. Role of 15-lipoxygenase/15-hydroxyeicosatetraenoic acid in hypoxia-induced pulmonary hypertension. *J Physiol Sci: JPS*. 2012;62:163–172.
39. Duan JJ, Cai J, Guo YF, Bian XW, Yu SC. Aldh1a3, a metabolic target for cancer diagnosis and therapy. *Int J Cancer*. 2016;139:965–975.
40. Farias JG, Herrera EA, Carrasco-Pozo C, Sotomayor-Zarate R, Cruz G, Morales P, Castillo RL. Pharmacological models and approaches for pathophysiological conditions associated with hypoxia and oxidative stress. *Pharmacol Ther*. 2016;158:1–23.
41. Mol M, Regazzoni L, Altomare A, Degani G, Carini M, Vistoli G, Aldini G. Enzymatic and non-enzymatic detoxification of 4-hydroxynonenal: methodological aspects and biological consequences. *Free Radic Biol Med*. 2017;111:328–344.
42. Semen K, Yelisseyeva O, Jarocka-Karpowicz I, Kaminskyy D, Solovey L, Skrzydlewska E, Yavorskyi O. Sildenafil reduces signs of oxidative stress in pulmonary arterial hypertension: evaluation by fatty acid composition, level of hydroxynonenal and heart rate variability. *Redox Biol*. 2016;7:48–57.
43. Chen CH, Ferreira JC, Gross ER, Mochly-Rosen D. Targeting aldehyde dehydrogenase 2: new therapeutic opportunities. *Physiol Rev*. 2014;94:1–34.
44. Marshall JD, Bazan I, Zhang Y, Fares WH, Lee FJ. Mitochondrial dysfunction and pulmonary hypertension: Cause, effect, or both. *Am J Physiol Lung Cell Mol Physiol*. 2018;314:L782–L796.
45. Otera H, Ishihara N, Mihara K. New insights into the function and regulation of mitochondrial fission. *Biochim Biophys Acta*. 2013;1833:1256–1268.
46. Chen KH, Dasgupta A, Lin J, et al. Epigenetic dysregulation of the dynamin-related protein 1 binding partners mid49 and mid51 increases mitotic mitochondrial fission and promotes pulmonary arterial hypertension: mechanistic and therapeutic implications. *Circulation*. 2018;138:287–304.
47. Ma C, Zhang C, Ma M, et al. Mir-125a regulates mitochondrial homeostasis through targeting mitofusin 1 to control hypoxic pulmonary vascular remodeling. *J Mol Med (Berl)*. 2017;95:977–993.
48. Kim D, Dai J, Park YH, Fai LY, Wang L, Pratheeshkumar P, Son YO, Kondo K, Xu M, Luo J, et al. Activation of epidermal growth factor receptor/p38/hypoxia-inducible factor-1alpha is pivotal for angiogenesis and tumorigenesis of malignantly transformed cells induced by hexavalent chromium. *J Biol Chem*. 2016;291:16271–16281.
49. Castro JP, Jung T, Grune T, Siems W. 4-hydroxynonenal (HNE) modified proteins in metabolic diseases. *Free Radic Biol Med*. 2017;111:309–315.
50. Gomes KM, Campos JC, Bechara LR, Queliconi B, Lima VM, Disatnik MH, Magno P, Chen CH, Brum PC, Kowaltowski AJ, et al. Aldehyde dehydrogenase 2 activation in heart failure restores mitochondrial function and improves ventricular function and remodeling. *Cardiovasc Res*. 2014;103:498–508.
51. Zhang Y, Mi SL, Hu N, Doser TA, Sun A, Ge J, Ren J. Mitochondrial aldehyde dehydrogenase 2 accentuates aging-induced cardiac remodeling and contractile dysfunction: role of AMPK, SIRT1, and mitochondrial function. *Free Radic Biol Med*. 2014;71:208–220.